



**Meshing:**

Named selections	No. of divisions	Bias factor
Upper lower	8	10
Upstream	30	25
Downstream	50	35
Span	250	35
BL affected zone	50	30
Tip	150	30
BL	200	35

The values used for generating fine mesh.

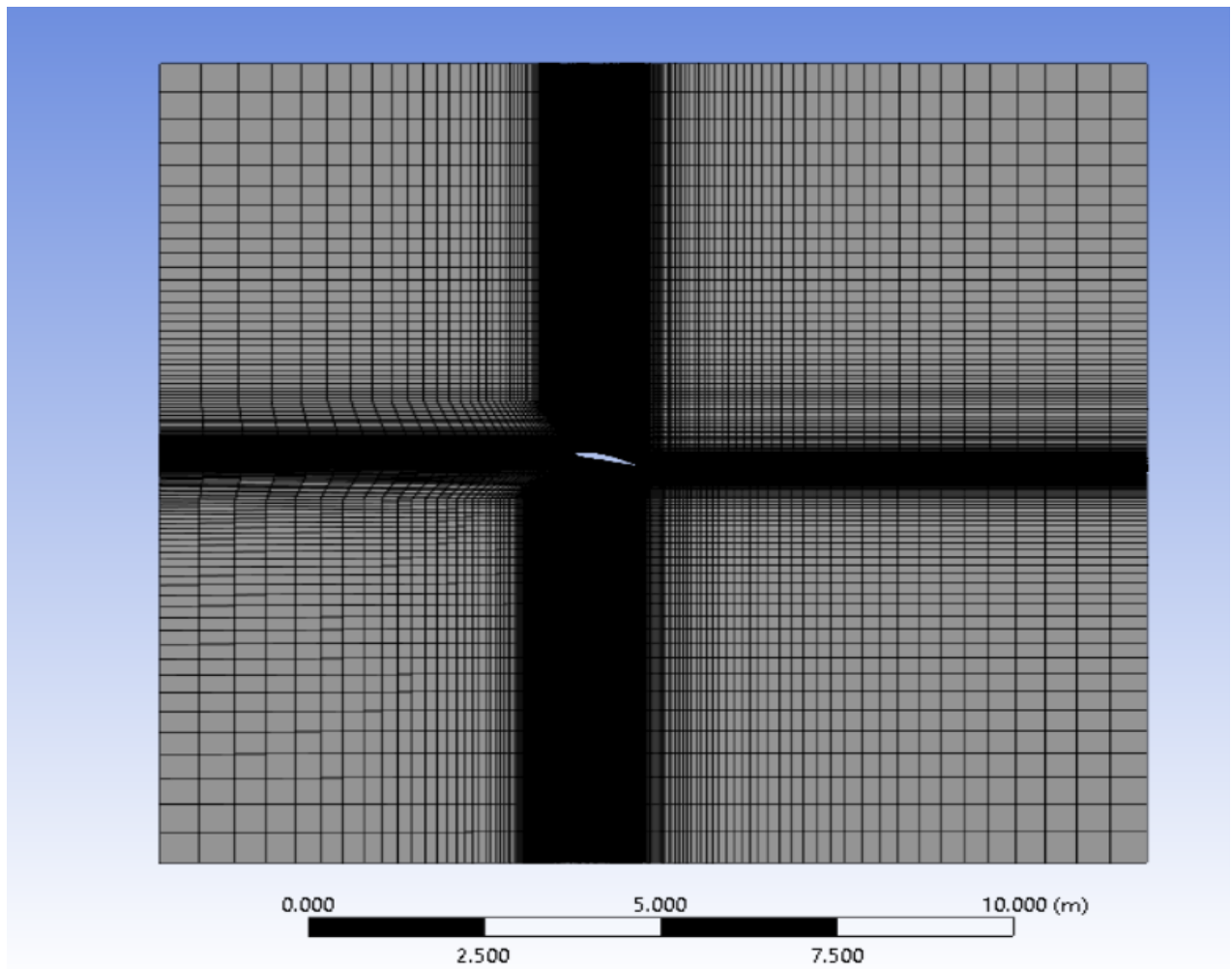


Fig. 2 overall meshed image.

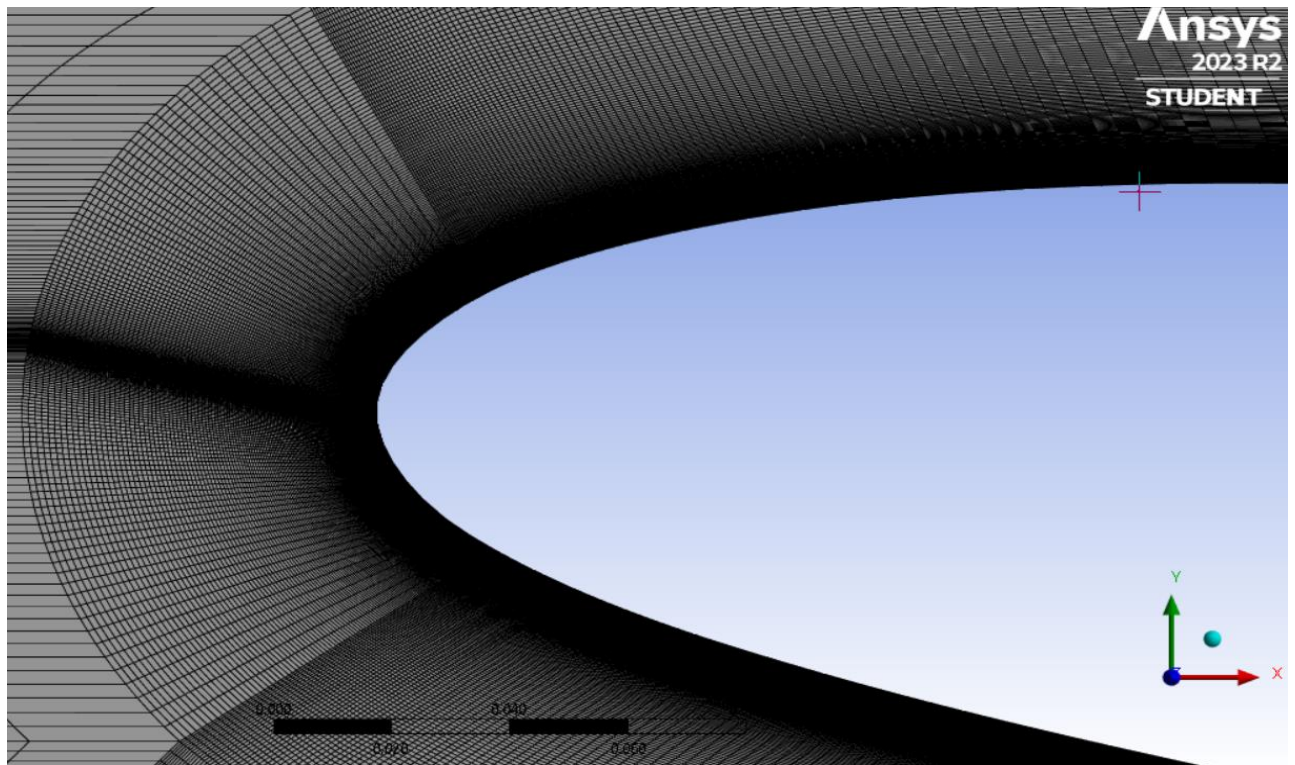


Fig. 3 Meshing at Leading edge of airfoil.

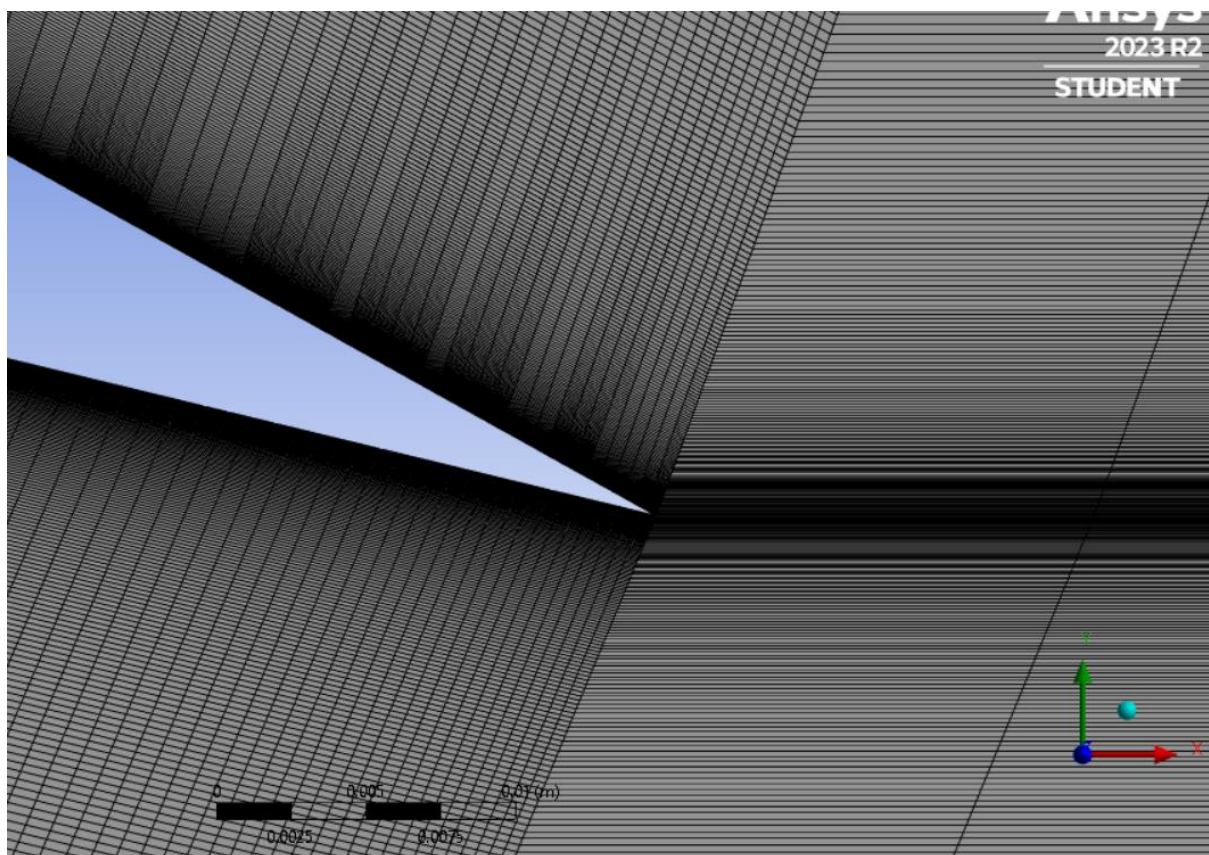


Fig.4 Meshing at Trailing Edge of airfoil.

## K-Omega Model:

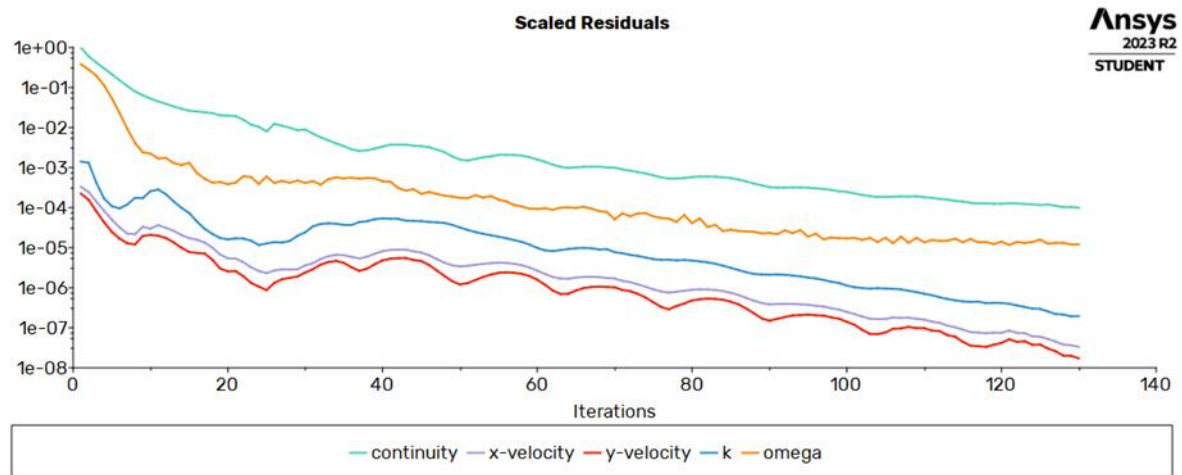


Fig. 5 Convergence plot for K-omega model.

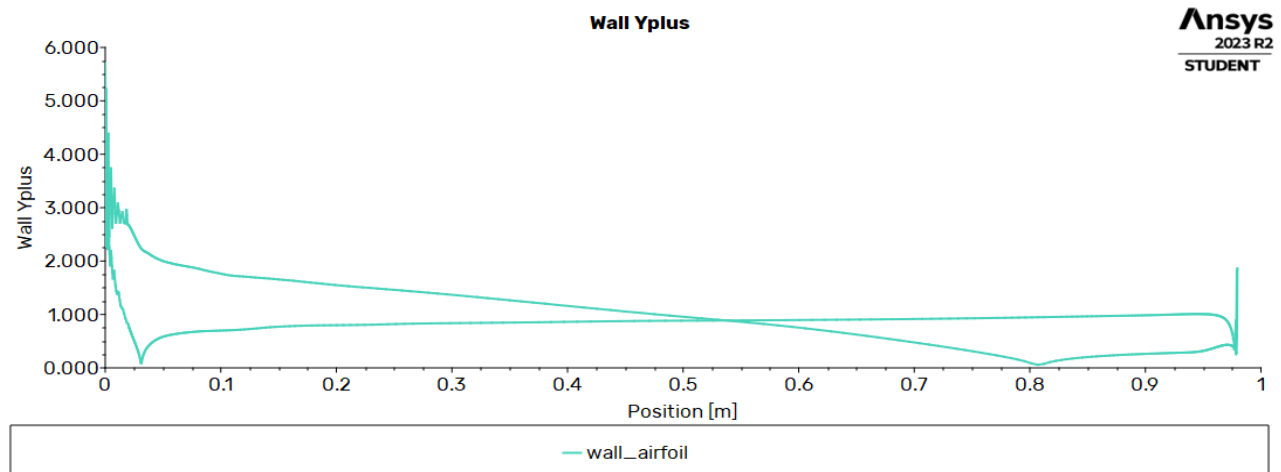


Fig. 6 Airfoil wall y plus values.

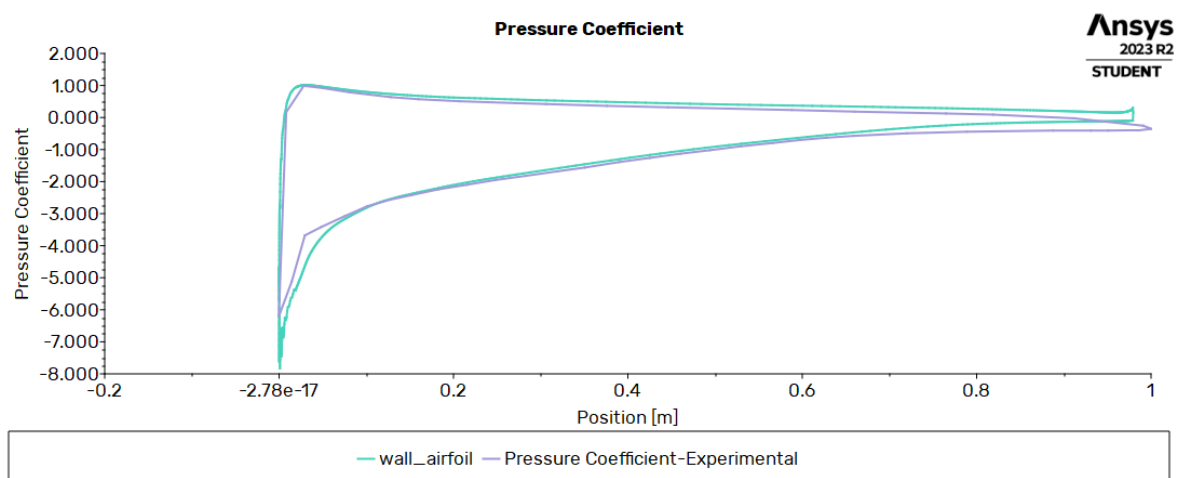


Fig. 7 Cp variation on upper and lower surfaces compared with experimental Cp variation.

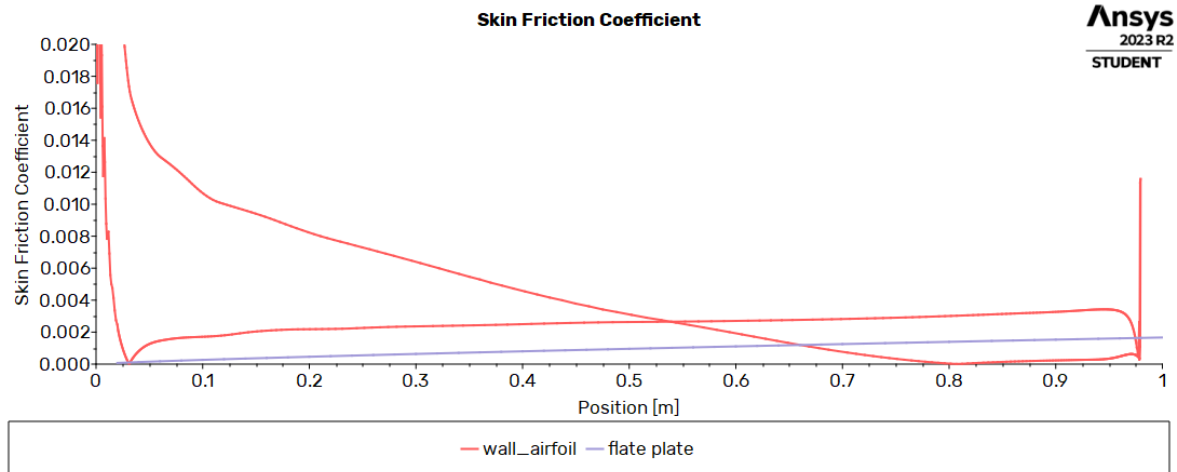


Fig. 8 Cf variation and comparison with Cf of flat plate relations.

K- $\omega$ model	
Cl_cfd	1.7146596
Cl_Airfoil data	1.65
Cd_cfd	0.043136545
Cd_Airfoil data	0.03

The values of Cl and Cd obtained in K-omega model.

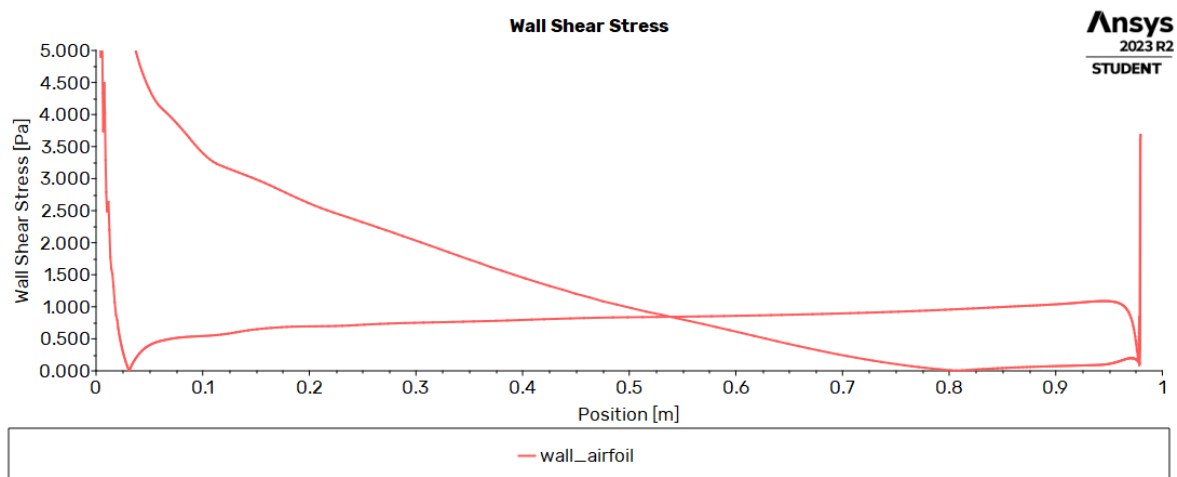


Fig. 9 Wall shear stress variation on airfoil wall by K-omega model. The flow separation length observed where value of wall shear stress reaches zero.

The value of flow separation from cfd was approximately 0.8 meters on upper surface.

The value of flow separation from experimental data was observed to be approx. 0.72 meters.

Further visualizations of flow separation can be done with the help of velocity vectors and contours.



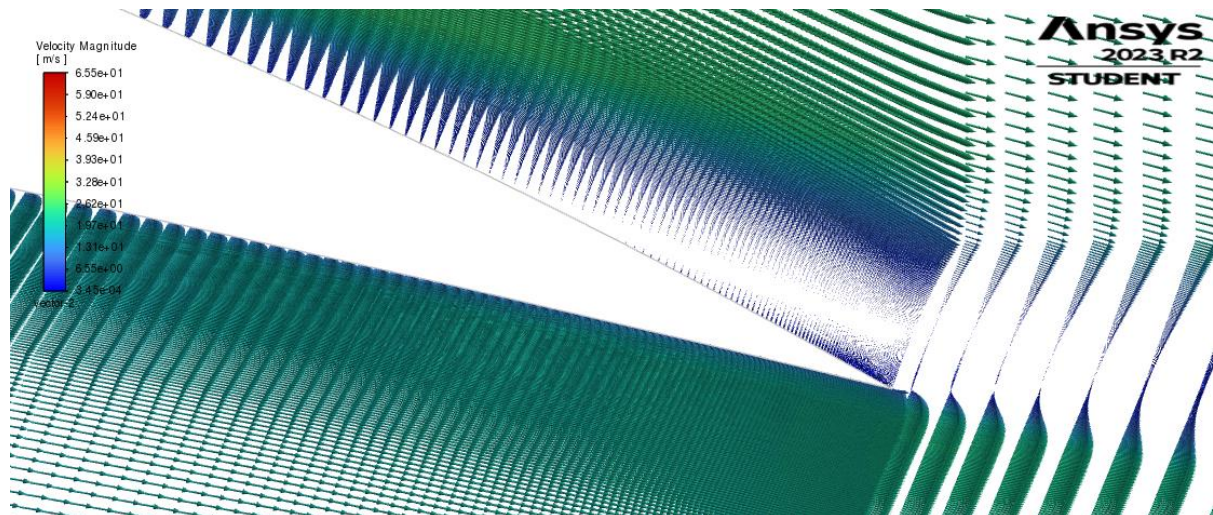


Fig. 10 velocity magnitude vector plot.

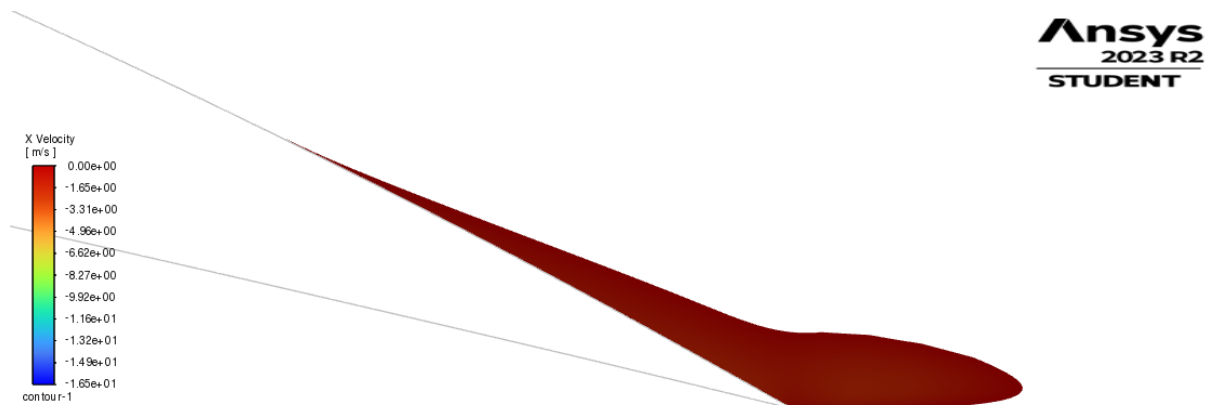


Fig. 11 negative x velocity contour. This shows from which point our recirculation starts.

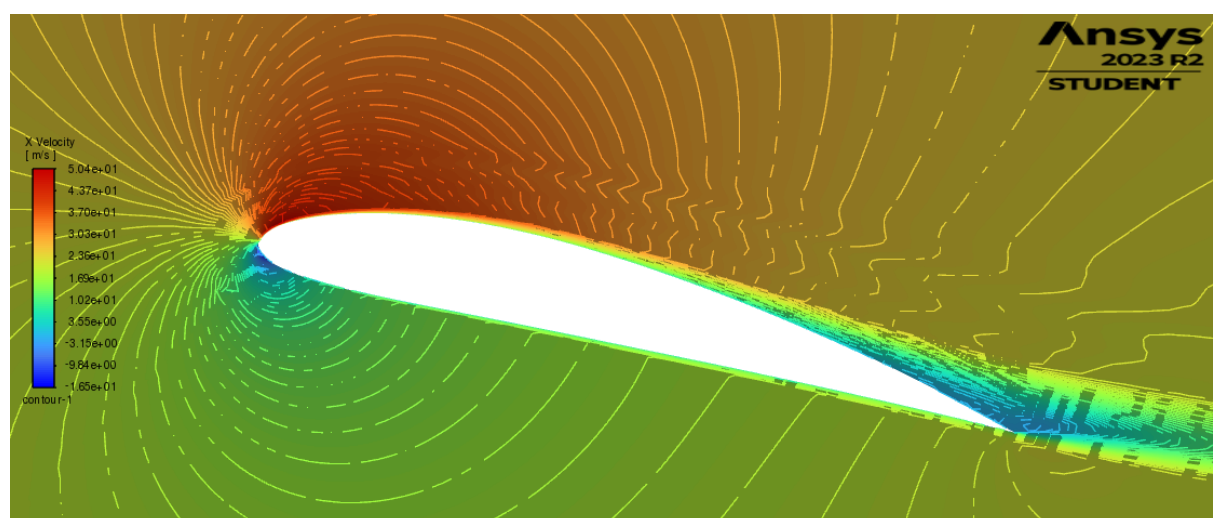


Fig.12 x velocity contours around airfoil wall.

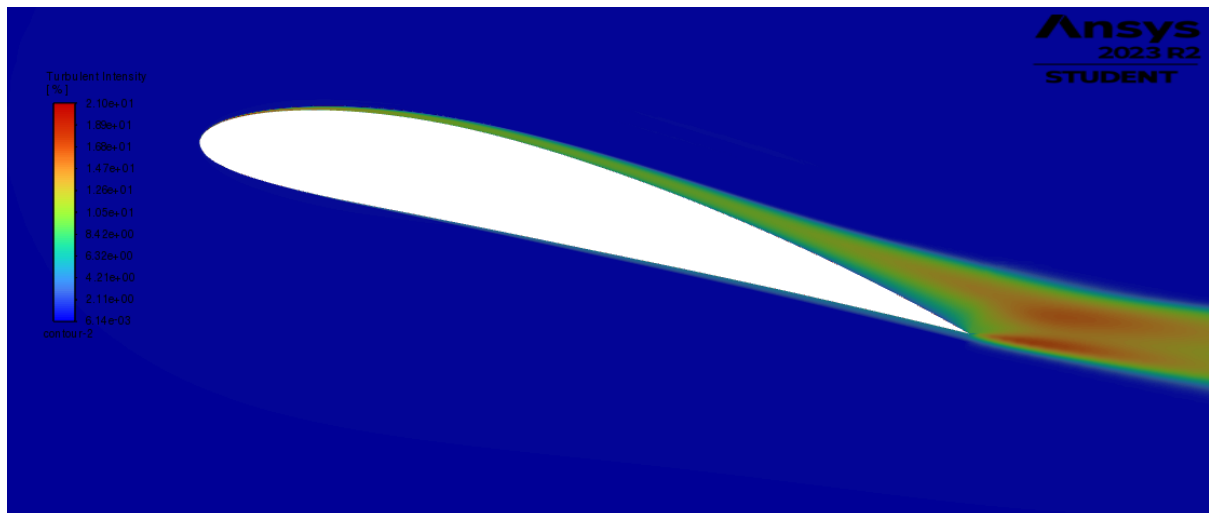


Fig.13 Turbulent intensity around airfoil. We can see increase in turbulent intensity after flow separation point and keeps on increasing along the trailing edge of the airfoil. It further decreases along the downstream of airfoil.

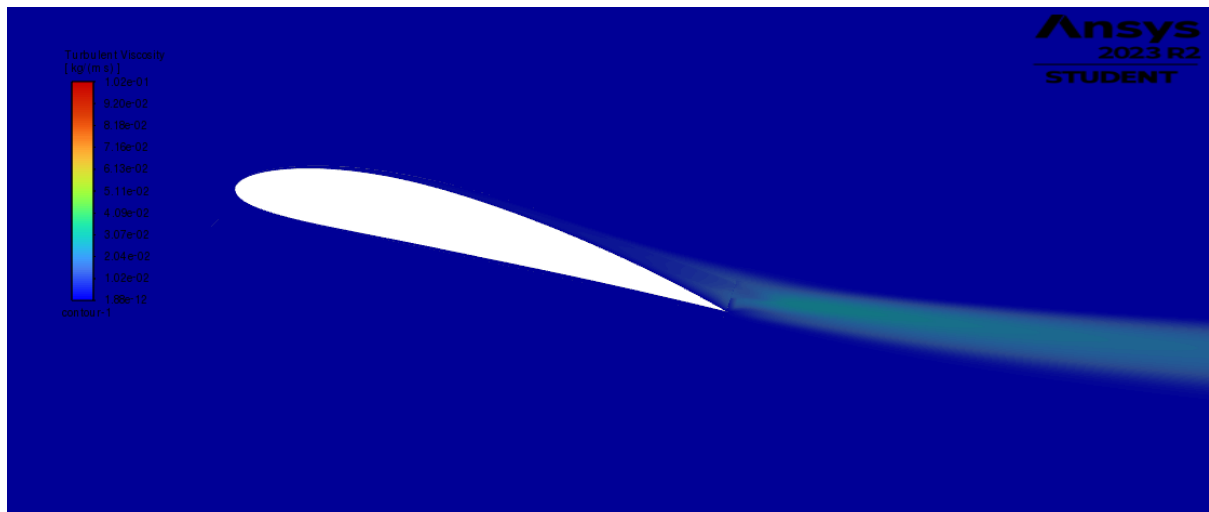


Fig.14 Turbulent viscosity along trailing edge.

## Spalart-Allamaras turbulence model:

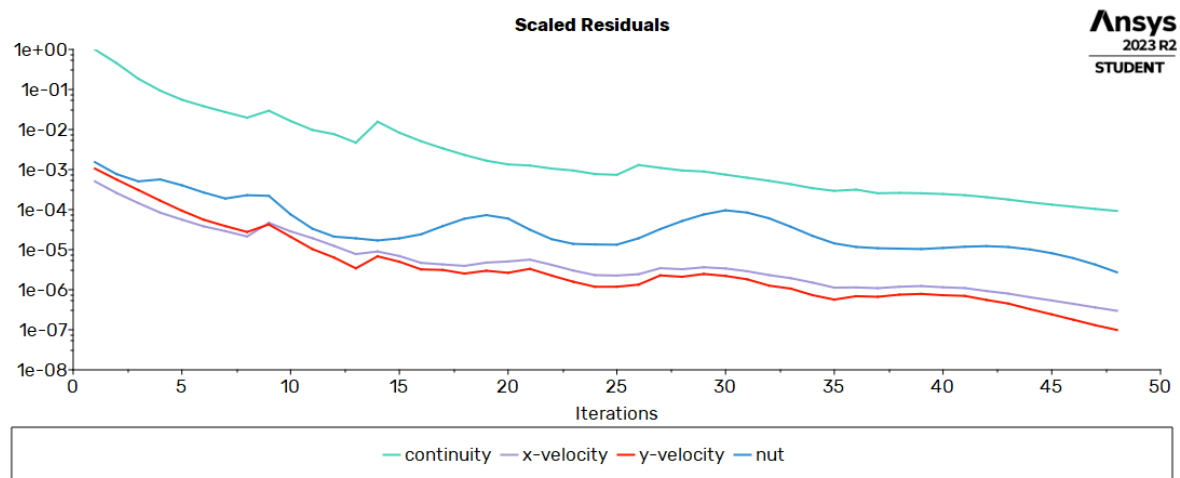


Fig. 15. Convergence plot for Spalart-Allamaras model.

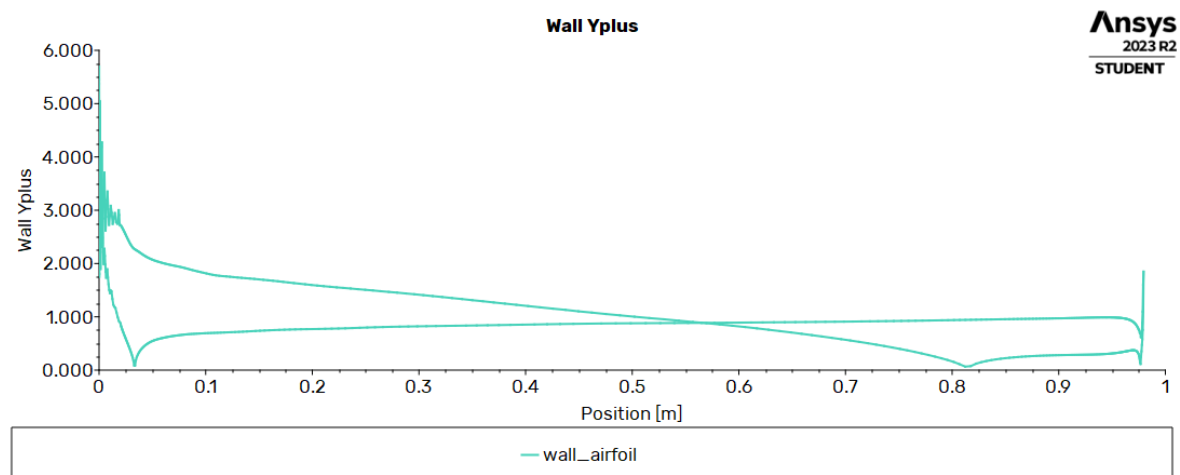


Fig. 16 Wall y plus values. This was derived from same mesh used for K-omega model.

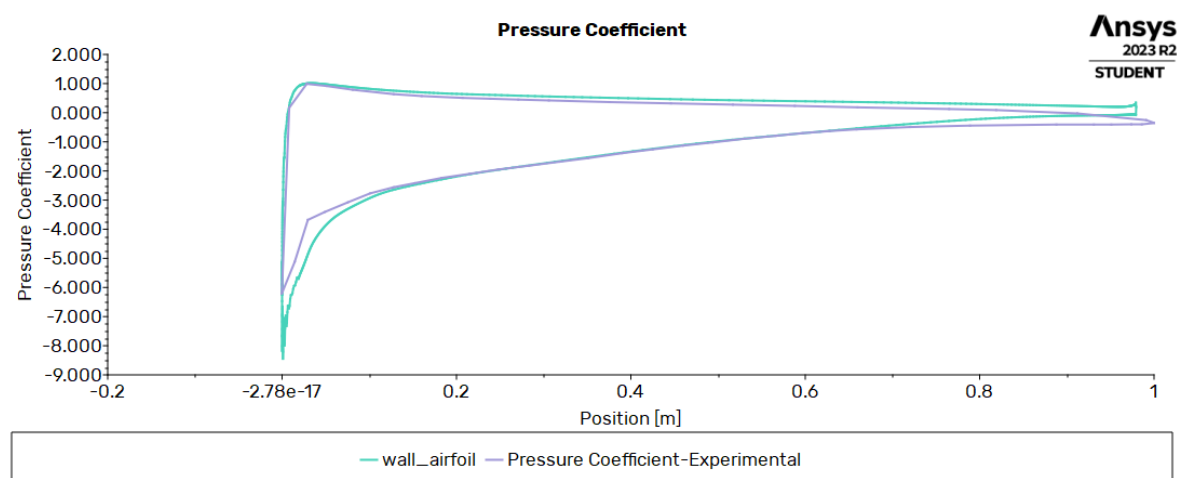


Fig. 17 Cp variation along airfoil wall and comparison with experimental Cp variation.



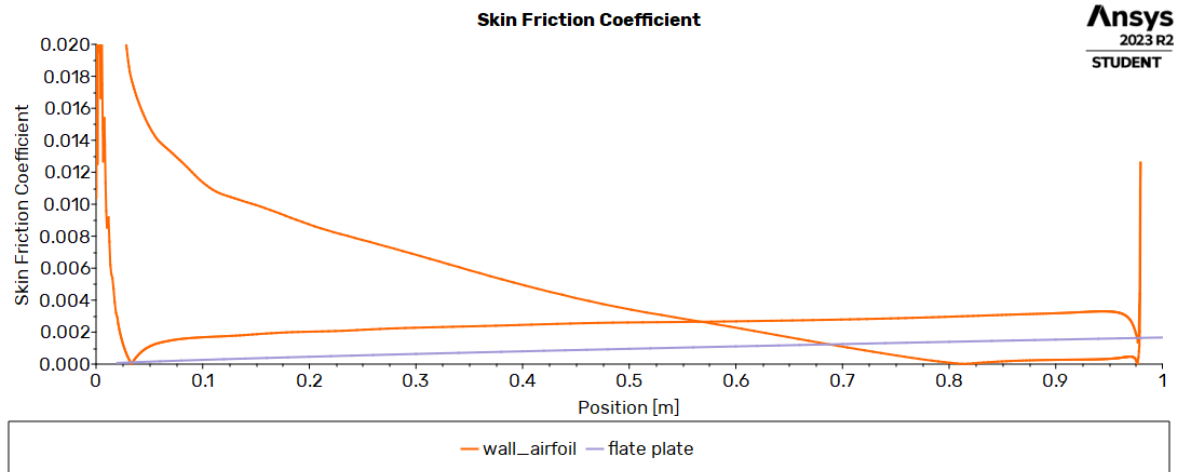


Fig. 18 Cf variation and comparison with Cf of flat plate relations.

Spalart-Allamaras	
Cl_cfd	1.8041823
Cl_Airfoil data	1.65
Cd_cfd	0.041202866
Cd_Airfoil data	0.03

Values of Cl and Cd obtained from Cfd by using Spalart-Allamaras model and average Cl and Cd by airfoil tools.

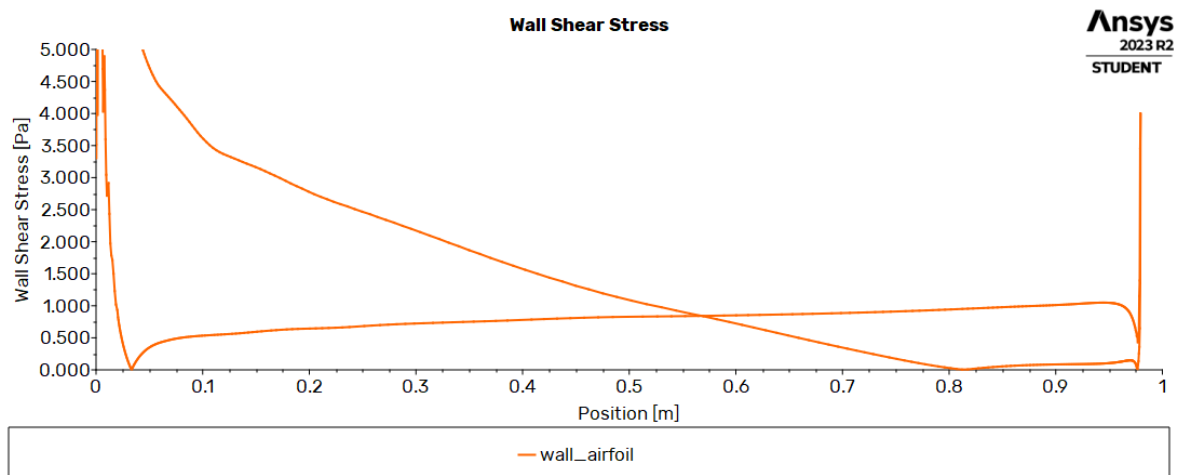


Fig. 19 Wall shear stress variation on airfoil wall by Spalart-Allamaras model. The flow separation length observed where value of wall shear stress reaches zero.

The value of flow separation from cfd was approximately 0.84 meters on upper surface.

The value of flow separation from experimental data was observed to be approx. 0.72 meters.

Model	Separation length
K- $\omega$	$\sim 0.8$ meters
Spalart-Allamaras	$\sim 0.84$ meters
Experimental	$\sim 0.72$ meters

Comparison of separation length from different models.

Further visualizations of flow separation can be done with the help of velocity vectors and contours.

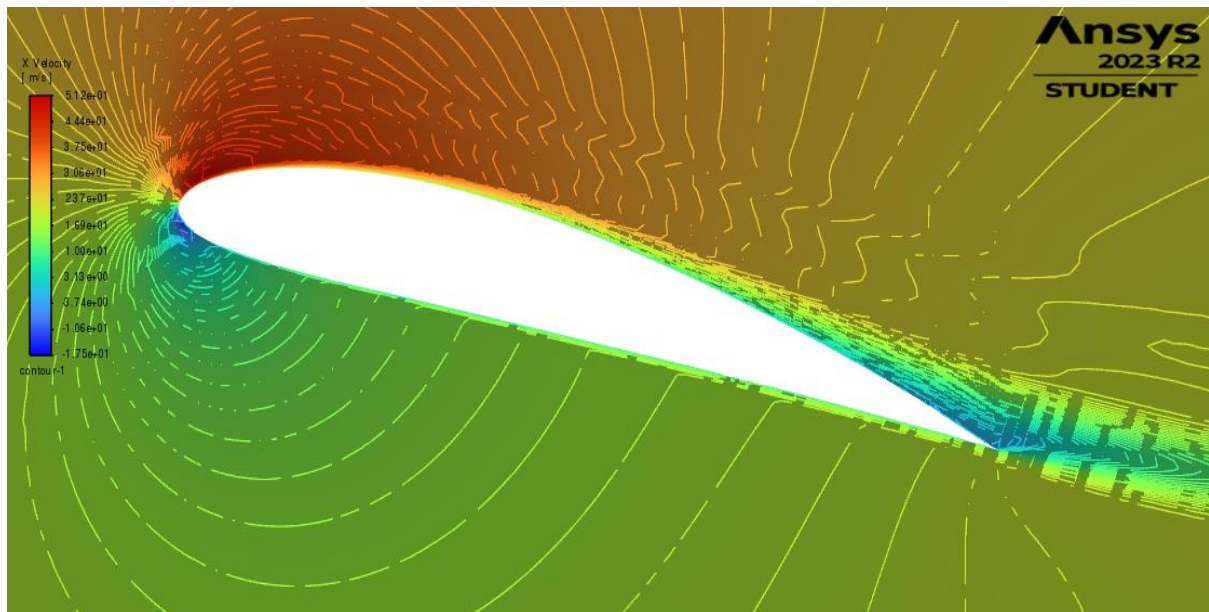


Fig.20 X velocity contours around airfoil.



Fig. 21 Negative X velocity zones showing recirculation around airfoil wall.

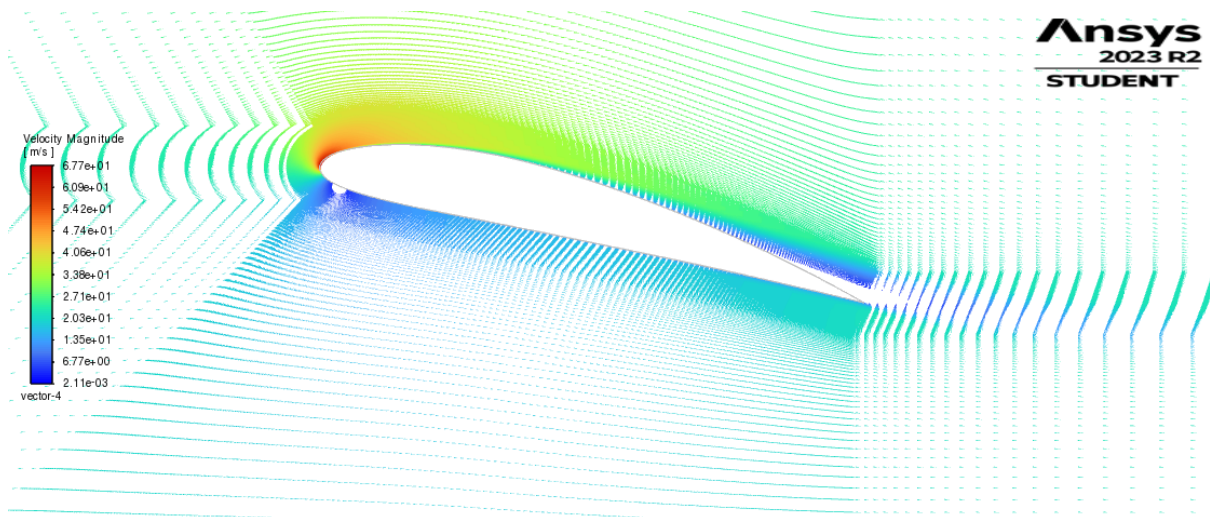


Fig. 22 Velocity vectors along airfoil showing two zones of very low velocity. One is along trailing edge where flow separation occurs. Another is below the leading edge.

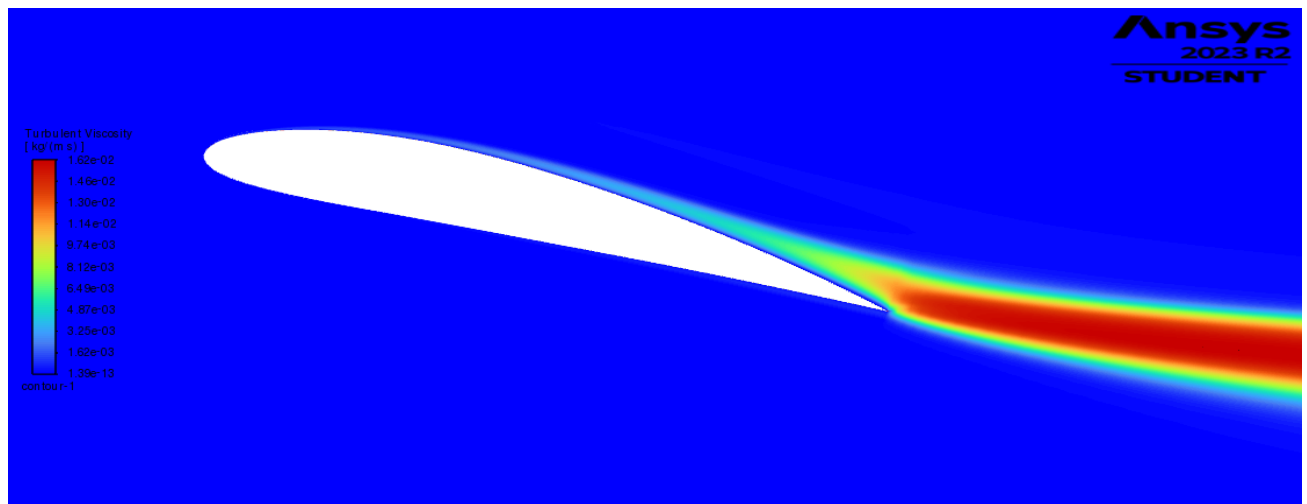


Fig. 23 Turbulent viscosity variation beyond trailing edge.

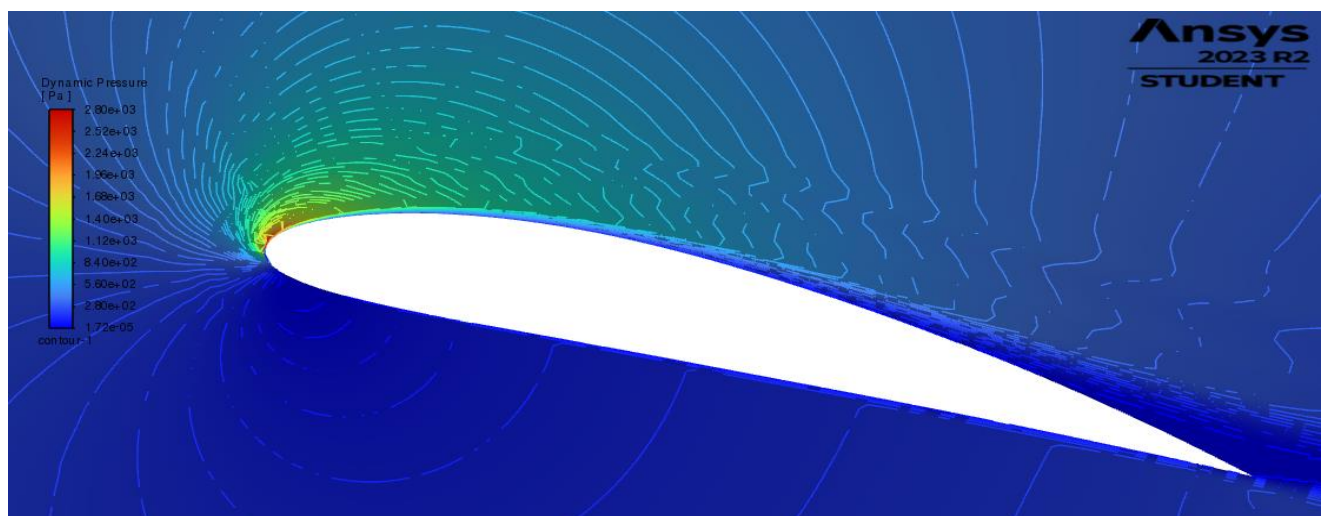


Fig. 24 Dynamic pressure variation along the wall.

## Discussions:

1. To utilize both the K- $\omega$  and Spalart Allmaras models effectively, the mesh refinement was done by using different no. of divisions and bias and checking for y plus values below unity. Validation involved ensuring Y+ values remained below unity across the majority of the airfoil surface.
2. The K- $\omega$  Model, featuring two transport equations, demonstrates superior accuracy compared to the Spalart Allmaras Model, which relies on a single transport equation. This is evident from the closer value of flow separation lengths obtained in K- $\omega$  models to experimental value.
3. Also from the convergence plots, we can see that because the Spalart Allmaras Model only has to deal with one equation, it tends to finish its calculations faster than the K- $\omega$  model, which has two equations to solve.
4. The value of lift coefficient and drag coefficient obtained by K- $\omega$  model was closer to the experimental values of average lift and drag coefficient, indicating its better representation of near-wall effects than the Spalart Allmaras model.
5. The Cp plots in both models were consistent with the experimental plot. Both had certain variability near the zones where turbulence or recirculation was observed. These zones were near the trailing edge and near the leading edge on lower surface. This can be due to large values of y plus near the ends of the airfoil wall. Further refinement on these values should lessen the variability.
6. The plot of flat plate skin friction coefficient was created from analytical equations of flat plates by varying Re. no. at different locations along chord. The lower surface showed similar variations of skin friction coefficient with flat plate. But upper surface was completely different from flat plate, and had lower values near trailing edge indicating lower wall stresses when compared to a flat plate upper surface.